

Crack problem for a long rectangular slab of superconductor under an electromagnetic force

You-He Zhou and Hua-Dong Yong

Key Laboratory of Mechanics on Western Disaster and Environment, Ministry of Education, Lanzhou, China
and Department of Mechanics, Lanzhou University, Lanzhou 730000, People's Republic of China

(Received 24 April 2007; published 28 September 2007)

The flux-pinning-induced singular stress field near the crack tips of a central crack is investigated. A model is presented in this paper to estimate the effect of the electromagnetic force on fracture behavior. The model provides an analytical tool for the investigation of the mechanical failure of superconductors. The stress intensity factors are computed for two activation processes. Numerical results obtained show that, generally, the stress intensity factor increases as the applied field becomes large during field descent. It is intended that the stress intensity factor analysis presented here be useful to researchers interested in cracking and mechanical failure of superconductors.

DOI: [10.1103/PhysRevB.76.094523](https://doi.org/10.1103/PhysRevB.76.094523)

PACS number(s): 46.25.Cc, 46.15.-x, 46.50.+a

I. INTRODUCTION

Bulk high temperature superconductors have been widely used in engineering, for example, frictionless bearing, motor components, etc.^{1,2} Recent progress in melt processing has enabled the production of large-grain Y-Ba-Cu-O superconductors with high critical current density (J_c) values,³ and trapped fields up to 12.2 T were obtained at 22 K on the surface of single YBCO disks (with Ag and Zn additions).⁴ However, the low tensile strength of these materials limits their field trapping capability. The mechanical stability can be threatened by the tensile stress generated during the activation process.⁵ Thus, more and more researchers have paid attention to the mechanical properties of the bulk superconductors. An unusually large magnetostriction in a single crystal was reported by Ikuta *et al.*⁶ They proposed a quantitative model which reproduced the observations very well in terms of internal forces arising from flux pinning. The flux-pinning-induced stress and strain in a long circular cylindrical superconductor were analyzed by Johansen,⁷ who discussed in detail two common magnetization processes: (1) a full cycle of the applied magnetic field after zero-field cooling and (2) a field reduction to zero after field cooling.

In the preceding articles, the effect of a crack was not considered when the deformation and stress were investigated. It has been reported that cracking occurs in a large single-grain bulk superconductor when the applied field was decreased from 10 to 0 T at 50 K.⁸ Owing to their brittleness, superconductors have a tendency to develop microcracks during fabrication process. When a cracked superconductor is subjected to a large electromagnetic force, the high stress concentration may initiate crack growth and eventually lead to fracture.⁹ Thus, it would be exceedingly useful to account for the fracture induced by the electromagnetic force. The formation and propagation of microcrack in melt-processed superconductors have been reported.^{10,11}

In this paper, a major effort is made to examine the effect of the electromagnetic force arising from flux pinning on the fracture behavior based on the assumption presented in Ref. 12, in which demagnetization effects are negligible and the slab is isotropic. In the present study, the calculations are restricted to the Bean model. To make the problem math-

ematically tractable, the total forces exerted on the boundary replace the body forces. Then, the Fourier transform technique is used to reduce the problem to the solution of a singular integral equation, which is solved numerically. In the subsequent sections, the stress intensity factors are obtained and discussed for decreasing field after zero-field cooling and field reduction after field-cooling conditions. The final section presents the conclusions of this paper.

II. PROBLEM STATEMENT AND BASIC EQUATIONS

Consider a center-situated Griffith crack of length $2a$ in an infinitely long slab of width $2h$ with reference to the rectangular coordinate system x, y, z (see Fig. 1). The slab is placed in a parallel magnetic field oriented parallel to the z axis and the crack lies in the x - y plane.

In order to calculate the stress intensity factors at crack tips, a relatively simple model is developed, in which the slab is isotropic. The slab is assumed to be infinite in the z direction, and therefore, demagnetization effects are negligible. In this model, the length of the crack is assumed to be much smaller than the width of the slab, i.e., $a \ll h$. Therefore, the crack exerts negligibly small disturbance to the shielding currents. Similar to the approach adopted by Johansen to determine flux density in a slab with rectangular cross section, the flux penetrates equally to all the edges, and the shielding currents that flow in loops are equidistant from the external boundary (see Fig. 2).¹³

The electromagnetic forces arising from flux pinning are body forces. The body forces have been given in the form

$$f_y = -\frac{1}{2\mu_0} \frac{\partial}{\partial y} B(y)^2. \quad (1)$$

For a crack problem under body force loading, it is generally quite difficult to determine the stress intensity factor and to obtain the effect of the electromagnetic force on the fracture behavior. Therefore, choose a uniform stress σ_b as equivalent to the body forces acting on the x - z plane. Integrating the body forces along the y axis, the uniform total force is given by

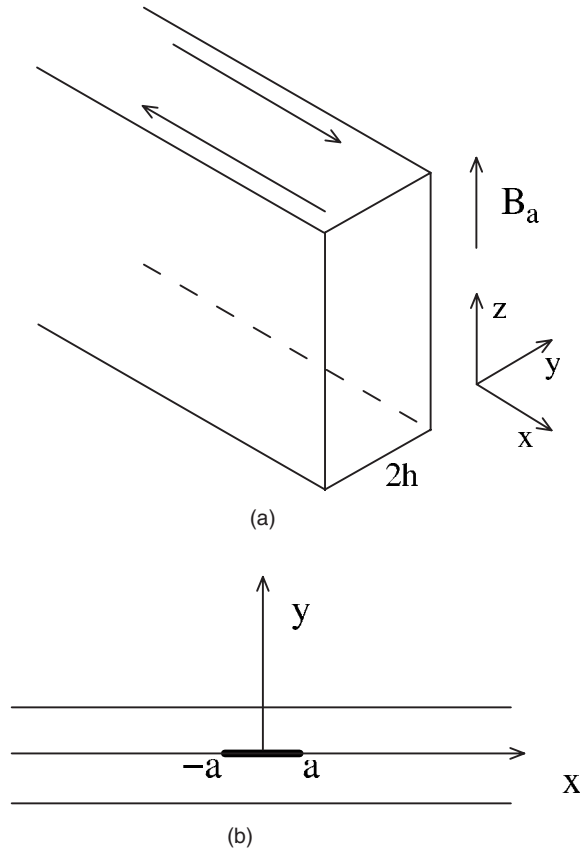


FIG. 1. Sketch of a rectangular slab superconductor placed in a magnetic field B_a . (a) Coordinate system for slab and flow of J_c in the slab. (b) Rectangular slab superconductor containing a crack parallel to the boundary.

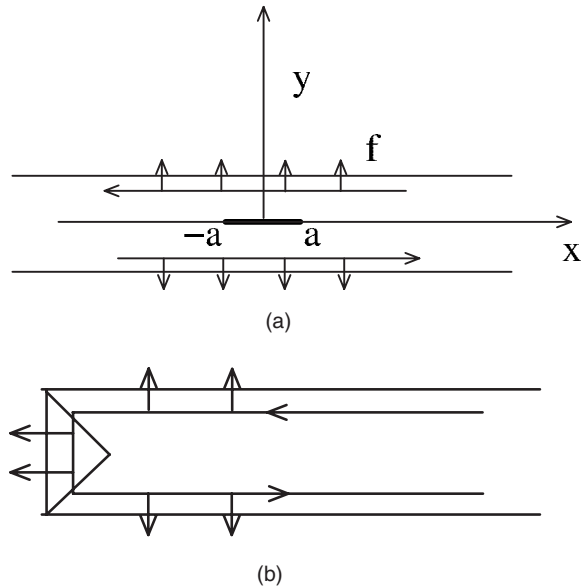


FIG. 2. Pinning-induced body forces and current in the cross sectional plane. (a) Body forces acting on the slab. (b) Triangular part containing body forces.

$$\sigma_b = \int_0^h f_y(y) dy = \frac{1}{2\mu_0} [B(0)^2 - B_a^2]. \quad (2)$$

Interestingly, the total force only depends on the magnetic field at $y=0$ and $y=h$. In addition, the body forces f_x have little effect near the crack tip and are neglected for the infinite slab. Since the problem is symmetric with respect to the x axis, it is sufficient to consider the upper plane for $y>0$. Through a proper superposition, the problem under consideration becomes finding a solution that satisfies the following boundary conditions:

$$\sigma_{yy}(x, h) = \sigma_{xy}(x, h) = 0, \quad -\infty < x < \infty, \quad (3)$$

$$\sigma_{xy}(x, 0) = 0, \quad -\infty < x < \infty, \quad (4)$$

$$\sigma_{yy}(x, 0) = -\sigma_b, \quad |x| < a, \quad (5)$$

$$v(x, 0) = 0, \quad |x| > a. \quad (6)$$

We will now investigate linear elastic solutions of the boundary value problem. A plane strain approach from linear elasticity theory can be applied.¹⁴ The governing equations for the slab may be expressed as

$$(\kappa + 1) \frac{\partial^2 u}{\partial x^2} + (\kappa - 1) \frac{\partial^2 u}{\partial y^2} + 2 \frac{\partial^2 v}{\partial x \partial y} = 0, \quad (7)$$

$$(\kappa - 1) \frac{\partial^2 v}{\partial x^2} + (\kappa + 1) \frac{\partial^2 v}{\partial y^2} + 2 \frac{\partial^2 u}{\partial x \partial y} = 0, \quad (8)$$

where $\kappa = 3 - 4\nu$.

Using Fourier transforms, we can obtain the following solutions:

$$u(x, y) = \frac{1}{2\pi} \int_{-\infty}^{+\infty} [(A_1 + A_2 y) e^{|s|y} + (A_3 + A_4 y) e^{-|s|y}] e^{isx} ds, \quad (9)$$

$$v(x, y) = \frac{1}{2\pi} \int_{-\infty}^{+\infty} [(B_1 + B_2 y) e^{|s|y} + (B_3 + B_4 y) e^{-|s|y}] e^{isx} ds. \quad (10)$$

In order to solve the unknowns $A_1 - A_4$ and $B_1 - B_4$, some manipulations are used to reduce the problem to a singular integral equation that can be solved numerically,

$$\begin{aligned} & \frac{4\mu}{(\kappa + 1)} \sum_{n=1}^{\infty} C_n U_{n-1}(r) - \frac{1}{2\pi} \frac{\mu}{(\kappa + 1)} \sum_{n=1}^{\infty} \int_{-1}^1 L(r, u) \frac{C_n T_n(u)}{\sqrt{1-u^2}} du \\ & = -\sigma_b, \end{aligned} \quad (11)$$

where C_n are unknown constants to be determined, and T_n and U_n are the Chebyshev polynomial functions of the first and second kind, respectively. Equation (11) can be solved by truncating the series and a collocation technique.¹⁵

After solving the unknowns coefficients C_n , the stress intensity factors can be defined and calculated as

$$K_I(a) = \lim_{x \rightarrow a} \sqrt{2(x-a)} \sigma_{yy}(x,0) = -\frac{4\sqrt{a}\mu}{\kappa+1} \sum_{n=1}^{\infty} C_n, \quad (12)$$

$$K_I(-a) = \lim_{x \rightarrow -a} \sqrt{2(-x-a)} \sigma_{yy}(x,0) = \frac{4\sqrt{a}\mu}{\kappa+1} \sum_{n=1}^{\infty} C_n. \quad (13)$$

To analyze the effects of the electromagnetic force, it is necessary to know the distribution of the flux density inside the superconductor. For simplicity, we adopt a relatively simple model, i.e., the Bean model. Accordingly, the critical current density J_c is independent of the magnetic field.

So far, major cracking due to pinning-induced compressive stress has not been reported.¹³ Cracking of samples was found for the reason that tensile stresses exceed the tensile strength of materials. Because tensile stresses occur during field reduction, the stress intensity factors are obtained for two magnetization processes: (1) a field reduction after zero-field cooling and (2) a field reduction to zero after field cooling.⁷ We define a characteristic field $B_p = \mu_0 J_c h$ equal to the full penetration field. The maximum applied field, which is denoted by \hat{B}_a , is chosen to be $\hat{B}_a \geq 2B_p$. For brevity, the following symbols are used in the following parts of this paper:

$$b_a = B_a/B_p, \quad \hat{b}_a = \hat{B}_a/B_p, \quad e = \frac{y}{h}, \quad (14)$$

$$\sigma_0 = \frac{B_p^2}{2\mu_0}, \quad K_0 = \sigma_0 \sqrt{\pi a}. \quad (15)$$

In the following parts, the solutions of the singular integral equation have been computed numerically, and the numerical results for the stress intensity factor are presented. Since the stress intensity factor at crack tip a is equal to that at crack tip $-a$ for the central crack, we will only present the numerical results at crack tip a .

III. DECREASING FIELD

A. Case (i): $\hat{B}_a - 2B_p < B_a < \hat{B}_a$

When the field is increased above the full penetration value, the critical current fills the entire cylinder. However, the direction of the critical current is reversed in the outer part of the slab as the applied field starts to decrease from its maximum value \hat{B}_a . It should be noted that in the outer part, the body forces are expansive, whereas they are compressive in the inner part, and therefore, the total forces applied on the crack faces may be tensile forces.

In this case, the flux density is piecewise linear and can be expressed as⁷

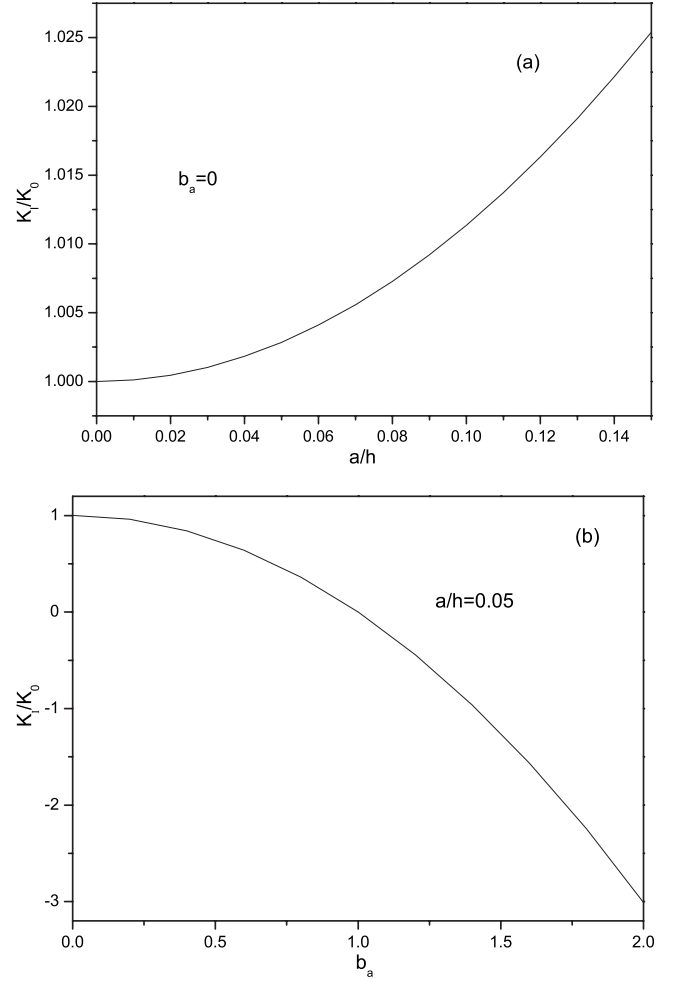


FIG. 3. (a) The crack length (a/h) dependence of stress intensity factor as the applied field is decreased from $\hat{b}_a=2$ to $b_a=0$. (b) Stress intensity factor as the applied field is decreased from $\hat{b}_a=2$ to $b_a=0$, for the case of $a/h=0.05$.

$$b = \hat{b}_a + e - 1, \quad 0 \leq e \leq e_0, \quad (16)$$

$$b = b_a + 1 - e, \quad e_0 \leq e \leq 1, \quad (17)$$

where $e_0 = 1 - (\hat{b}_a - b_a)/2$.

Figure 3(a) shows the effects of the crack length on the stress intensity factor as the field decreases from $2B_p$ to the remanent state $B_a=0$. Generally, it is expected that the stress intensity factor is greater when the crack length is longer for the same activation process.

Shown in Fig. 3(b) is the plot of the stress intensity factor while the applied field is reduced from $\hat{b}_a=2$ to $b_a=0$. When $b_a=0$, the maximum trapped flux is obtained in the remanent state. It can be found that the stress intensity factor decreases as b_a increases, and the stress intensity factor has a maximum at $b_a=0$, which implies that the highest cracking probability occurs at $b_a=0$. Notice that at $b_a=1$, the stress intensity factor is equal to 0. This clearly indicates that the total forces are expansion for $b_a < 1$, decrease, and then become

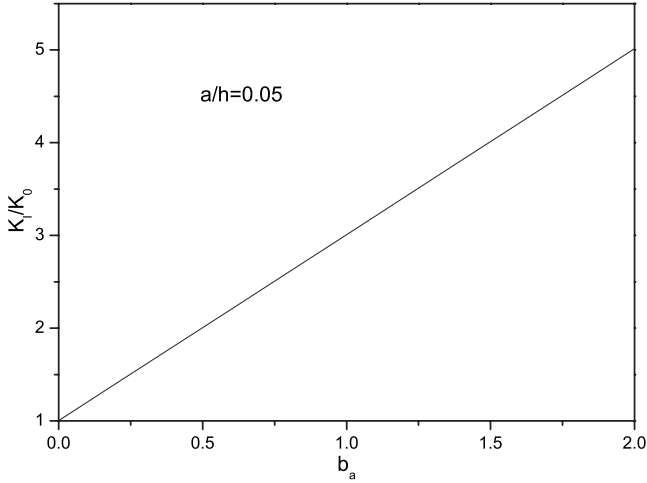


FIG. 4. Stress intensity factor as the applied field is decreased from $\hat{b}_a \geq 4$ to $b_a=0$, for the case of $a/h=0.05$.

compressive for $b_a > 1$. Moreover, while the stress intensity factor is negative, it implies crack closure.

B. Case (ii): $\hat{B}_a - 2B_p > B_a$

To satisfy the condition $\hat{B}_a - 2B_p > B_a$, the maximum applied field \hat{B}_a is assumed to be larger than $4B_p$. One can see that the current is reversed in the entire slab as the applied field is reduced by more than twice the full penetration field. Therefore, it is important to note that the body forces are all tensile and the total forces behavior becomes different with the previous case (i). The flux density yields the following expressions:

$$b = b_a + 1 - e, \quad 0 < e < 1. \quad (18)$$

Figure 4 shows the variations of the stress intensity factor during field descent after being first raised to $\hat{B}_a \geq 4B_p$. It is obvious that with the increasing of b_a , the stress intensity factor increases linearly. Since the body forces are all tensile, the stress intensity factor always has positive value. Compared to Fig. 3(b), here there is a larger stress intensity factor for the same b_a . Thus, the probability for cracking is greater in this case. It is worth noticing that the stress intensity factor at $b_a=2$ is five times as large as that at $b_a=0$. Choosing a proper field during field reduction is vital.

IV. FIELD COOLING

Compared to the pulsed field activation, the field-cooling method requires a much weaker field source to accomplish full activation. The method is cooling a HTS in a fixed magnetic field B_{fc} and then the applied field is removed, and a large part of the field remains trapped inside the superconductor. It is assumed that B_{fc} is also the flux density frozen in the superconductor when the subsequent field descent starts. Thus, the flux density can be defined as

$$b = b_{fc}, \quad 0 < e < e_0, \quad (19)$$

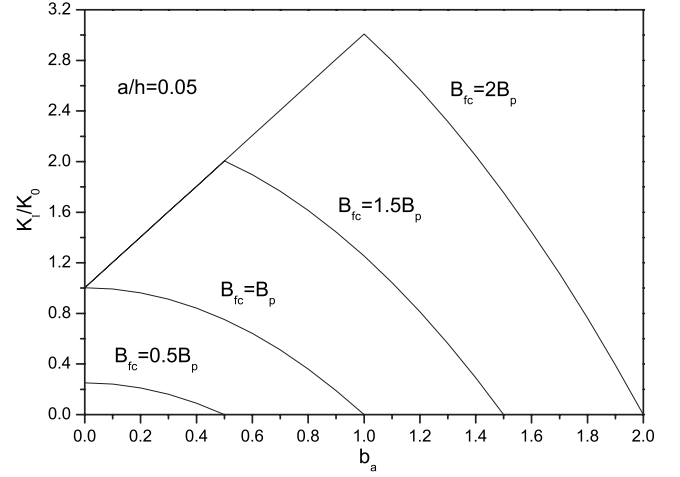


FIG. 5. Stress intensity factor profiles during field descent to the remanent state after field cooling with $b_{fc}=0.5, 1.0, 1.5, 2.0$.

$$b = b_a + 1 - e, \quad e_0 < e < 1, \quad (20)$$

where $e_0 = 1 - b_{fc} + b_a$.

The stress intensity factor at the crack tip as the applied field is reduced from b_{fc} to $b_a=0$ is plotted in Fig. 5. As we can see from the plot, there are striking differences between the cases when $b_{fc} > 1$ and $b_{fc} \leq 1$. When $b_{fc} \leq 1$, the stress intensity factor decreases with the increase of b_a . In other words, the crack growth is most likely to occur for the process of ramping down the applied field from b_{fc} to $b_a=0$. When $b_{fc} > 1$, the maximum stress intensity factor is generated as the applied field is reduced from b_{fc} to $b_{fc}-1$. Note that the stress intensity factor is greater when the applied field b_{fc} is higher. Thus, it is clear that in order to reach the goal of a given trapped field, we should use the lowest possible activation field.

V. CONCLUSION

The relatively simple model is inappropriate for the case that the length of the crack is not very small compared to the width of the slab. It is for this reason that the perturbation brought upon by the crack is no longer negligibly small. For the convenience of understanding the problem, we only discuss the central crack problem. However, knowing the length and location of the crack is imperative in predicting the highest cracking probability.

In this paper, the fracture behavior is investigated for a superconductor slab with a center-situated crack. We assume that the crack does not grow too large in size and the flow of the persistent current is only weakly perturbed. In addition, let the total forces applied on the boundary plane of the slab replace the body forces. The plane strain approach is used to find an exact solution. The calculations are carried out based on the simple Bean model. Several relations between the stress intensity factor and b_a are also presented.

The stress intensity factor behavior is discussed for field reduction. As expected, the stress intensity factor depends on the length of the crack. On the other hand, the stress intensity

factor can be reduced by decreasing the applied field. In other words, a lower applied field leads to a smaller stress intensity factor. It is clear that it is necessary to improve the mechanical strength at the same time when we make efforts to increase the trapped field.

We study the problem of a central crack in a long rectangular superconductor. However, some researchers have paid attention to the other topics of research on bulk

superconductors.^{16,17} We expect that more papers will be devoted to the studies of the magnetoelastic effects.

ACKNOWLEDGMENTS

This work was supported by the key fund of NSFC (No. 10532040, 90405005) and the Ph.D. Fund of the Ministry of Education of China (No. 20050730016).

-
- ¹F. C. Moon and P.-Z. Chang, *Appl. Phys. Lett.* **56**, 397 (1990).
²J. R. Hull, E. F. Hilton, T. M. Mulcahy, Z. J. Yang, A. Lockwood, and M. Strasik, *J. Appl. Phys.* **78**, 6833 (1995).
³T. Miyamoto, K. Nagashima, N. Sakai, and M. Murakami, *Physica C* **349**, 69 (2001).
⁴S. Gruss, G. Fuchs, G. Krabbes, P. Verges, G. Stöver, K.-H. Müller, J. Fink, and L. Schultz, *Appl. Phys. Lett.* **79**, 3131 (2001).
⁵Y. Ren, R. Weinstein, J. Liu, R. P. Sawh, and C. Foster, *Physica C* **251**, 15 (1995).
⁶H. Ikuta, N. Hirota, Y. Nakayama, K. Kishio, and K. Kitazawa, *Phys. Rev. Lett.* **70**, 2166 (1993).
⁷T. H. Johansen, *Phys. Rev. B* **60**, 9690 (1999).
⁸T. Miyamoto, K. Nagashima, N. Sakai, and M. Murakami, *Physica C* **340**, 41 (2000).
⁹M. Tomita and M. Murakami, *Physica C* **392-396**, 493 (2003).
¹⁰P. Diko, M. Ausloos, and R. Cloots, *Physica C* **235-240**, 359 (1994).
¹¹P. Diko, *Supercond. Sci. Technol.* **11**, 68 (1998).
¹²T. H. Johansen, *Phys. Rev. B* **59**, 11187 (1999).
¹³T. H. Johansen, *Supercond. Sci. Technol.* **13**, 121 (2000).
¹⁴S. Timoshenko and J. N. Goodier, *Theory of Elasticity* (McGraw-Hill, New York, 1951).
¹⁵F. Erdogan and B. H. Wu, *J. Therm. Stresses* **19**, 237 (1996).
¹⁶Y. Yang and X. J. Zheng, *J. Appl. Phys.* **101**, 113922 (2007).
¹⁷X. F. Gou, Y. Yang, and X. J. Zheng, *Appl. Math. Mech.* **25**, 297 (2004).